Polarization-dependent characteristics of a racetrack waveguide resonator fabricated by ion exchange in K9 glass

Xiuyou Han (韩秀友)[1,2], Feng Liu (刘 峰)[1,2], Fufei Pang (庞拂飞)[1,2], Fenghong Chu (初凤红)[1,2], Haiwen Cai (蔡海文)[1], Ronghui Qu (瞿荣辉)[1], and Zujie Fang (方祖捷)[1]

[1]*Shanghai Institute of Optics and Fine Mechanics, Chinese Academy of Sciences, Shanghai 201800*

[2]*Graduate School of the Chinese Academy of Sciences, Beijing 100039*

Received March 9, 2006

A racetrack waveguide resonator filter was fabricated by ion exchange technology in K9 optical glass. The filter responses of the waveguide resonator were measured with two polarized input lightwaves. The polarization-dependent characteristics of the waveguide resonator were analyzed, and the results of effective indices of $n_{\rm TE} = 1.5721$ and $n_{\rm TM} = 1.5548$, coupling ratios of $r_{\rm TE} = 0.731$ and $r_{\rm TM} = 0.761$, and losses of $\alpha_{\rm TE} = 4.35$ dB/cm and $\alpha_{\rm TM} = 6.05$ dB/cm were obtained for transverse electric (TE) and transverse magnetic (TM) modes, respectively. The causes of large loss and effective index differences between TE and TM modes were discussed.

OCIS codes: 130.0130, 130.3120, 130.2790, 230.5750.

Integrated optical waveguide ring resonators have received considerable attention because of their outstanding filter functions and compact structures. They can be used as tunable wavelength selective filters and a core part of sensitive sensors[1,2], and many characteristics of ring resonators, such as thermo-optical tuning, dispersion compensation, polarization-dependence, have been investigated widely[3−6].

For its merits of economy and simplicity, the ion exchange technology has been used to fabricate good quality optical waveguide devices. A few kinds of waveguide ring resonator structures have also been fabricated by ion exchange technology[7−9]. The polarization characteristics play important roles in waveguide device application, which may be utilized to fulfill novel effect or may deteriorate the function of device[10]. As far as we know, there have not been publications about the polarization-dependent characteristics of ion-exchanged glass waveguide ring resonator.

In this paper, a racetrack resonator filter was fabricated by ion exchange technology with mixed molten salt of $AgNO_3$ and KNO_3 in K9 optical glass. The filter responses of the waveguide resonator were measured with two polarized input lightwaves. The polarization-dependent characteristics of the waveguide resonator were analyzed.

A waveguide racetrack resonator filter with two "bus waveguides" coupled to a closed racetrack loop is illustrated in Fig. 1. The racetrack structure has advantages over conventional ring structure where ring is coupled to input and output waveguides via a "point contact". The length of coupling section in the racetrack resonator can be adjusted alone to attain a desired coupling ratio without requiring a very small gap, which decreases the difficulty of fabrication. The filter response of the racetrack resonator is similar to the functionality of Fabry-Perot filter, with output Z corresponding to transmission, and output Y corresponding to reflection of Fabry-Perot configuration. According to the usual transmission matrix approach[11], the transmission from port Y and port Z of the racetrack resonator can be expressed as

$$T_{\rm Y} = \frac{r[1+\gamma-2\sqrt{\gamma}\cos(nkL)]}{1+r^2\gamma-2r\sqrt{\gamma}\cos(nkL)}, \qquad (1)$$

$$T_{\rm Z} = \frac{(1-r)^2\sqrt{\gamma}}{1+r^2\gamma-2r\sqrt{\gamma}\cos(nkL)}, \qquad (2)$$

where two couplers are supposed to be the same with intensity coupling coefficient of r, as shown in Fig. 1, n is the effective index of the waveguide, k is the wave vector in vacuum, $\gamma = \exp(-\alpha L)$ is the intensity loss factor experienced in a round trip, α is the transmission loss coefficient per unit length, $L = 2\pi R + 2L_{\rm c}$ is the resonator circumference, R is the curvature radius and $L_{\rm c}$ is the straight waveguide length in the coupling region.

The resonance will occur under condition of $nkL = m\pi$ $(m = 0, 1, 2, \cdots)$, giving the maximum and minimum transmissions for port Y and port Z as

$$T_{\rm Y}|_{\rm max\,/\,min} = \frac{r(1\pm\sqrt{\gamma})^2}{(1\pm r\sqrt{\gamma})^2}, \qquad (3)$$

$$T_{\rm Z}|_{\rm min\,/\,max} = \frac{(1-r)^2\sqrt{\gamma}}{(1\pm r\sqrt{\gamma})^2}. \qquad (4)$$

The resonant wavelengths can be given as $\lambda_m = nL/m$ and $\lambda_m = nL/(2m+1)$ for port Y and port Z,

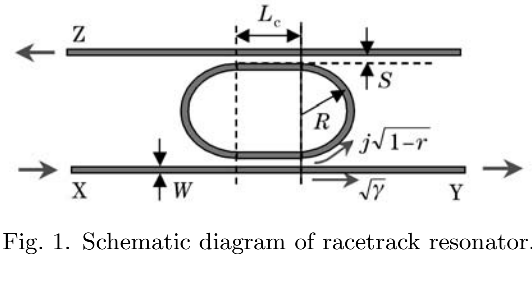

Fig. 1. Schematic diagram of racetrack resonator.

respectively. And the free spectrum range (FSR) can be written as

$$\mathrm{FSR} = \frac{\lambda_m^2}{nL}. \tag{5}$$

From Eqs. (3) and (4), the logarithmic contrast can be deduced as

$$C_{\mathrm{Y}} = 10\log(\frac{T_{\mathrm{Y}}|_{\max}}{T_{\mathrm{Y}}|_{\min}}) = 20\log\left[\frac{(1+\sqrt{\gamma})(1-r\sqrt{\gamma})}{(1-\sqrt{\gamma})(1+r\sqrt{\gamma})}\right], \tag{6}$$

$$C_{\mathrm{Z}} = 10\log(\frac{T_{\mathrm{Z}}|_{\max}}{T_{\mathrm{Z}}|_{\min}}) = 20\log\frac{1+r\sqrt{\gamma}}{1-r\sqrt{\gamma}}. \tag{7}$$

The parameters n, r, and α for transverse electric (TE) and transverse magnetic (TM) modes will have different values if polarization-dependent characteristics are to be considered, giving different resonant wavelengths and different FSRs for the two modes.

The waveguide racetrack resonator was fabricated in K9 optical glass by ion exchange technology with mixed molten salt of $AgNO_3$ and KNO_3. KNO_3 was introduced to dilute $AgNO_3$ in order to control the variation of refractive index easily[12]. The mask of the racetrack resonator was designed with the following parameters, R = 1.2 mm, L_c = 0.5 mm with the total length L = 8.54 mm, the waveguide width W= 6 μm, and the spacing between the coupler waveguides S = 4 μm. Fabrication procedure of the waveguide resonator was as follows. Radio-frequency (RF) sputtering was used to deposit a 150-nm-thick layer of titanium onto the glass surface. With Shipley 1805 photosensitive resist as the mask, the resonator pattern was etched into the titanium using H_2SO_4 as the etching acid at 85 °C in water bath. The ion exchange was performed in a mixed molten salt of $AgNO_3$ and KNO_3 with molar ratio 2% and 98% for 2 hours at 340 °C. In the process, one-step ion exchange was used. After ion exchange, the titanium layer was removed and the substrate's edges were polished properly.

Figure 2 shows the micrographs of the waveguide resonator and the coupling region, where we can clearly see that the two waveguides of coupler are separated. The fabricated strip width was about 7.5 μm, and the spacing between the waveguides inside the coupling region was about 2.5 μm due to the expanding in the photo-lithography processing and the lateral diffusion during the ion exchange. The effective depth of the ion exchanged waveguide was estimated to be 3.40 μm by M-line measurement of the planar layer[13]. Some cream-colored bands can be observed along the strip waveguide sides. This phenomenon was reported before and was explained mainly to be the electrolytic deposition of metallic silver beneath the edge of a titanium mask[14].

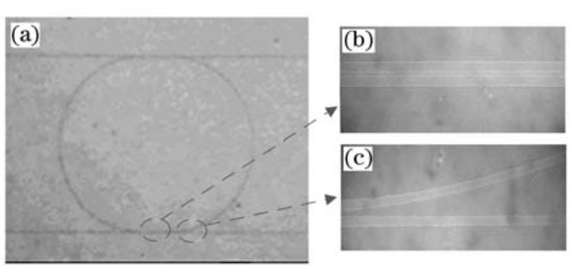

Fig. 2. Micrograph of the ion exchanged racetrack waveguide resonator. (a) Integral structure; (b) parallel straight waveguides of the coupling region; (c) diverging waveguides of the coupling region.

The filter responses of the waveguide resonator were measured with differently polarized input lightwaves. The measurement setup is shown in Fig. 3. Light from a tunable laser is coupled into one end of the straight waveguide using a lensed fiber. A polarization controller is used to adjust the polarization state of the input light. Signal collection and wavelength scan are controlled synchronously by computer. Then the polarization-dependent responses of the racetrack waveguide resonator can be measured.

Figure 4 shows the transmission spectra of port Z for TE and TM polarizations, where one can see six resonant peaks in the span both for TE and TM modes, which are the typical characteristics of ring resonator. Another important feature in Fig. 4 is that the TM peak shifts a little towards the longer wavelength direction than the corresponding TE peak. To see the difference clearlier, the margin between TE and TM modes is depicted in Fig. 5 with the largest value of 4 dB, showing that the ring resonator will change the polarization state of input lightwave.

From Fig. 4, one can read that the average FSRs for TE and TM modes are 0.179 and 0.181 nm, respectively. According to Eq. (3), the effective refractive indices of TE and TM modes can be calculated as 1.5721 and 1.5548, respectively. It is reasonable that the effective index of TE mode is higher than that of TM mode, as usually observed in planar waveguides, and also in strip waveguides with effective waveguide depth smaller than its width. Figure 6 highlights the deviation of the resonant wavelength between TE and TM modes, showing that the resonant wavelength of TM mode is larger than that of TE

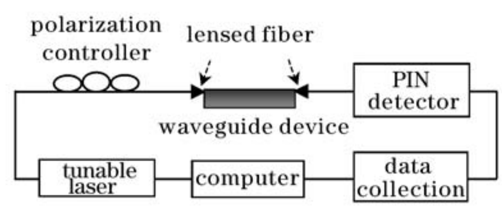

Fig. 3. Measurement setup for device characterization.

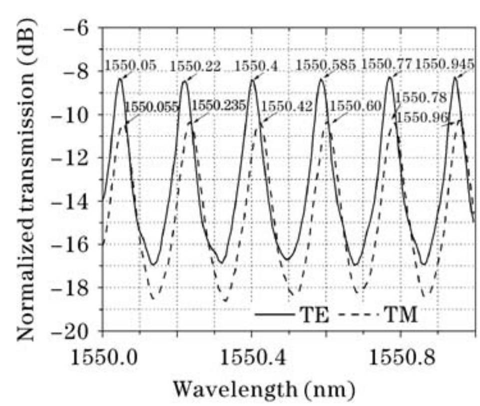

Fig. 4. Measured TE and TM polarization filter responses from port Z.

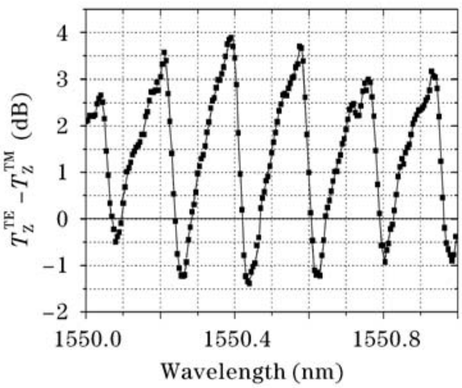

Fig. 5. Transmission intensity difference between TE and TM polarizations from port Z.

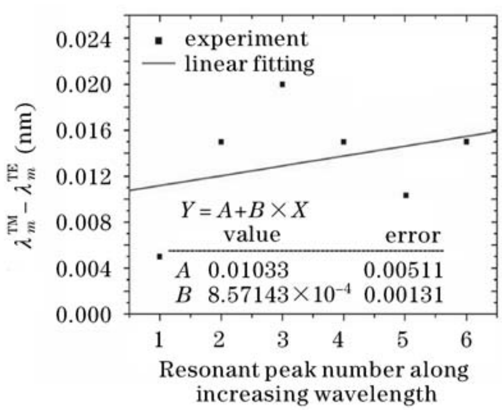

Fig. 6. Deviation of resonant wavelength between TE and TM polarizations.

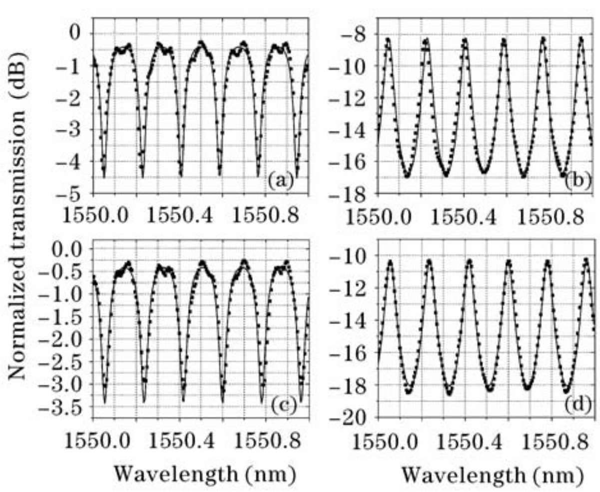

Fig. 7. Filter responses of the racetrack resonator for different polarization modes. (a) Port Y, TE mode; (b) port Z, TE mode; (c) port Y, TM mode; (d) port Z, TM mode.

mode. The data seem divergent, but a linear fitting can be made approximately with slope of 8.6×10^{-4} nm/FSR, which indicates the group index dispersion in some degree, though further work is needed for more precise measurement.

The transmission responses of TE and TM modes at ports Y and Z are depicted in Fig. 7 respectively, where the square symbols represent experiment results and the solid curves represent the fitted results based on Eqs. (1) and (2). From the fitting, the coupling ratios are obtained to be $r_{\mathrm{TE}} = 0.731$ and $r_{\mathrm{TM}} = 0.761$, and the loss factors to be $\gamma_{\mathrm{TE}} = 0.425$ and $\gamma_{\mathrm{TM}} = 0.304$, giving transmission loss coefficients of $\alpha_{\mathrm{TE}} = 4.35$ dB/cm and $\alpha_{\mathrm{TM}} = 6.05$ dB/cm.

The transmission loss of the ion exchanged glass waveguide resonator is large relatively. There may be several factors to cause it, such as bending radiation loss, transition loss at the junctions between straight and curved waveguides, material absorption loss and surface scattering loss. Among them, the surface scattering loss caused by the irregularity of the strip waveguide side and flaw of waveguide surface is supposed to be the main factor for the one-step ion exchanged waveguide. The transmission loss could be decreased when the waveguide is buried by two-step ion exchange[15] or field-assisted annealing[16]. The fact that the transmission loss of TM mode is larger than the one of TE mode is attributed to two causes. Firstly, TM mode has a lower effective index than TE mode, thus resulting in a more widely spread mode field and larger intensity distribution at the interface between the waveguide surface and the air, which will make the scattering loss increase. The second, the silver deposition bands at the sides of strip waveguide, as mentioned above, will cause larger TM mode attenuation by evanescent field in the silver metal. Further investigations are needed to improve the loss performances.

The polarization dependence of this waveguide resonator is severe relatively ($\Delta n = n_{\mathrm{TE}} - n_{\mathrm{TM}} = 0.0173$), which may be caused by the residual stress in the ion exchanged region and the asymmetrical refractive index profile after one-step ion exchange. To decrease the polarization dependence, further processing should be taken, for example, annealing[16] or two-step ion exchange[17], which would make the stress distribution uniform and refractive index profile symmetrical. On the other hand, in the filed of utilizing polarization function, large polarization dependence can be produced by using exchanging ion pair with large ion radius difference[18].

In conclusion, a racetrack resonator filter has been fabricated in K9 optical glass by ion exchange technology with mixed molten salt of $AgNO_3$ and KNO_3. The filter responses for different polarization modes were measured and the polarization-dependent characteristics were analyzed. The causes of large loss and effective index differences between TE and TM modes have been discussed. Further work is being done for reducing the loss and investigating the polarization property, and the research result will be reported later. The ion exchanged glass waveguide resonator can be used in filter and sensor fields and new functions may be realized by combination with other waveguide structures.

This work was supported by the Optical Science and Technology Foundation of Shanghai Technology Committee under Grant No. 022261009. X. Han's e-mail address is hanxiuyou@mail.siom.ac.cn.

References

1. B. E. Little, S. T. Chu, H. A. Haus, J. Foresi, and J.-P. Laine, J. Lightwave Technol. **15,** 998 (1997).
2. D. Culemann, A. Knuettel, and E. Voges, IEEE J. Sel. Top. Quantum Electron. **6,** 730 (2000).

3. C. K. Madsen, G. Lenz, A. J. Bruce, M. A. Capuzzo, L. T. Gomez, T. N. Nielsen, and I. Brener, Opt. Lett. **24,** 1555 (1999).
4. P. Katila, P. Heimala, and J. Aarnio, Electron. Lett. **32,** 1005 (1996).
5. M.-K. Chin, C. Xu, and W. Huang, Opt. Express **12,** 3245 (2004).
6. W. R. Headley, G. T. Reed, S. H. A. Liu, and M. Paniccia, Appl. Phys. Lett. **85,** 5523 (2004).
7. R. G. Walker and C. D. W. Wilkinson, Appl. Opt. **22,** 1029 (1983).
8. W. J. Wang, S. Honkanen, S. I. Najafi, and A. Tervonen, Electron. Lett. **28,** 1976 (1992).
9. G. Li and K. A. Winick, in *Proceedings of Conference on Lasers and Electro-Optics (CLEO) 2004* **1,** 2 (2004).
10. A. M. F. Morichetti and M. Martinelli, Opt. Lett. **29,** 2785 (2004).
11. A. Yariv, Electron. Lett. **36,** 321 (2000).
12. R. V. Ramaswamy and R. Srivastava, J. Lightwave Technol. **6,** 984 (1988).
13. X. Han, F. Pang, F. Chu, H. Cai, R. Qu, and Z. Fang, Journal of Optoelectronics·Laser (in Chinese) (to be published).
14. R. G. Walker, C. D. W. Wilkinson, and J. A. H. Wilkinson, Appl. Opt. **22,** 1923 (1983).
15. J. Z. Zou, F. Zhao, and R. T. Chen, Appl. Opt. **41,** 7620 (2002).
16. K. Liu and E. Y. B. Pun, IEEE Photon. Technol. Lett. **17,** 76 (2005).
17. A. Brandenburg, J. Lightwave Technol. **4,** 580 (1986).
18. T. Findakly, Opt. Eng. **24,** 244 (1985).